IRSTI 29.27.17 https://doi.org/10.26577/RCPh20259214

S.N. Hsseinimotlagh , A. Shakeri*
Department of Physics, Shiraz Branch, Islamic Azad University, Shiraz, Iran
*e-mail: Abuzar.shakeri6845@gmail.com

Improving proton therapy of breast cancer via AuNPs injection

Beam therapy plays an important role in the treatment of cancer, which is the most common and successful form of treatment used after surgery. In proton therapy, proton beam (PB) particles irradiate the tumor. To enhance the treatment of breast tumor, it is possible to inject gold nanoparticles (AuNPs) into the tumor at the same time as irradiating the PB. The aim of this paper is simulation of breast tumors treatment using PBs and injecting AuNPs with different concentrations, simultaneously. Therefore, we introduce the breast phantom (BP), then irradiate it with a proton pencil beam which is also injected with AuNPs at the same time. To show the enhancement of the absorbed dose in the tumor, we use the MCNPX.2.6 code. Findings of our simulations show that the location of the Bragg's peak within the tumor shifts to higher depths with increasing energy. Also, by injecting AuNPs in different amounts of 10, 25, 50 and 75mg/ml with PB irradiation simultaneously, the rate of absorbed dose increases up to 1.75% compared to the non-injected state. Our results also show that optimal range of proton energy that creates Bragg peaks within the tumor is 52 up to 65 MeV, which causes the creation of spread out of Bragg peak. It should be noted that the amount of absorbed dose is affected by quantities such as total stopping power, average Coulomb scattering angle, CSDA and straggling range. This work offers new insights based on the use of AuNPs in the treatment of breast cancer through proton therapy and indicates that the addition of AuNPs is a promising strategy to increase the killing of cancer cells while irradiating fast PBs. In fact, the results of this study confirm the ability of AuNPs to enhance treatment by increasing the absorbed dose in breast tumors using proton therapy.

Keywords: tumor, proton therapy, breast, enhancement.

С.Н. Хсейнимотлаг, А.Шәкери*
Физика кафедрасы, Шираз филиалы, Ислам Азад университеті, Шираз қ., Иран
*e-mail: Abuzar.shakeri6845@gmail.com

Сүйектің ауруын протонды терапиямен AuNPs енгізу арқылы емдеуді жетілдіру

Сәулелік терапия – қатерлі ісіктерді емдеуде хирургиялық араласудан кейін қолданылатын ең кең таралған және табысты әдістердің бірі. Протондық терапияда ісікке протондық сәуле шоғымен (ПШ) әсер етіледі. Сүт безі ісігін емдеудің тиімділігін арттыру үшін ісікке алтын нанобөлшектерін (AuNPs) енгізу ПШ-мен бір уақытта жүргізілуі мүмкін. Бұл жұмыстың мақсаты — сүт безі ісіктерін емдеу үрдісін әртүрлі концентрациядағы AuNPs енгізу арқылы және ПШ-мен қатар симуляциялау. Осы мақсатта сүт безінің фантомы (СБФ) ұсынылып, ол протон сәулесімен бірге AuNPs енгізіле отырып сәулелендіріледі. Ісіктегі жұтылған дозаның күшеюін көрсету үшін MCNPX.2.6 коды қолданылды.

Біздің модельдеу нәтижелері көрсеткендей, энергия артқан сайын Брегг шыңының орналасуы ісік ішінде тереңірек аймақтарға жылжиды. Сонымен қатар, AuNPs 10, 25, 50 және 75 мг/мл концентрациясында ПШ-мен бірге енгізілгенде, жұтылған доза мөлшері AuNPs енгізілмеген жағдаймен салыстырғанда 1,75%-ға дейін артады. Сондай-ақ, ісік ішінде Брегг шыңын туындататын протон энергиясының оңтайлы диапазоны 52-ден 65 МэВ-қа дейінгі аралықта орналасқаны анықталды, бұл кеңейтілген Брегг шыңының пайда болуына әкеледі. Жұтылған доза мөлшері толық тоқтату қуаты, орташа Кулон шашырау бұрышы, CSDA және шашырау ауқымы секілді параметрлерге тәуелді болады. Бұл зерттеу алтын нанобөлшектерін сүт безі ісігін протондық терапия арқылы емдеуде қолданудың жаңа мүмкіндіктерін көрсетіп, AuNPs енгізу рак жасушаларын жою тиімділігін арттырудың келешегі зор стратегиясы екенін дәлелдейді.

Түйін сөздер: ісік, протондық терапия, сүт безі, тиімділікті арттыру.

С.Н. Хсейнимотлаг, А.Шәкери*
Кафедра физики, филиал в Ширазе, Исламский университет Азад, г. Шираз, Иран
*e-mail: Abuzar.shakeri6845@gmail.com

Улучшение протонной терапии рака молочной железы путем введения золотых наночастиц (AuNPs)

Лучевая терапия играет важную роль в лечении онкологических заболеваний и является наиболее распространённым и эффективным методом после хирургического вмешательства. В протонной терапии опухоль облучается протонным пучком (ПП). Для повышения эффективности лечения рака молочной железы возможно одновременное введение в опухоль золотых наночастиц (AuNPs) во время облучения ПП. Целью настоящей работы является моделирование процесса лечения опухолей молочной железы с применением ПП и одновременным введением AuNPs в различных концентрациях. В рамках исследования создан фантом молочной железы, который подвергается облучению тонким протонным пучком с одновременным введением AuNPs. Для оценки увеличения поглощённой дозы в опухоли использовалась программа MCNPX.2.6.

Результаты моделирования показывают, что положение пика Брегга в пределах опухоли смещается вглубь при увеличении энергии. Также было установлено, что при одновременном введении AuNPs в концентрациях 10, 25, 50 и 75 мг/мл с ПП происходит увеличение поглощённой дозы до 1,75% по сравнению с вариантом без введения наночастиц. Кроме того, установлено, что оптимальный диапазон энергии протонов, при котором формируется пик Брегга внутри опухоли, составляет от 52 до 65 МэВ, что приводит к формированию расширенного пика Брегга. Следует отметить, что на величину поглощённой дозы оказывают влияние такие параметры, как полная тормозящая способность, средний угол кулоновского рассеяния, диапазон CSDA и флуктуации пробега. Данное исследование открывает новые перспективы применения AuNPs в лечении рака молочной железы с помощью протонной терапии и подтверждает перспективность введения AuNPs как стратегии повышения эффективности уничтожения раковых клеток при облучении высокоэнергетическим ПП.

Ключевые слова: опухоль, протонная терапия, молочная железа, усиление.

Introduction

Today, hadron therapy with heavy charged particles is a modern technique in radiotherapy, so that it has physical and radiobiological advantages and in general has useful clinical properties. Physically, because of optimal absorbed dose distribution of heavy charged particles, healthy tissues can be significantly protected from unwanted damage, which in turn reduces side effects and secondary cancers. In addition, from a radiobiological point of view, the RBE of these particles is higher than that of photons, thereby increasing the efficiency of killing cancer cells and increasing the probability of tumor control. Thus, this technique is considered the preferred and definitive method in terms of cancer treatment. From a DNA damage perspective, it can be argued that cancer treatment uses the proton hadron beam to damage the DNA of cancer cells without destroying healthy cells. However, in X-ray therapy, nearby non-cancerous cells are also destroyed.

In recent years, the use of high-Z NPs is presented for tumor activation in order to increase absorbed dose inside it and different studies are performed on the effects of NPs such as gold, silver, platinum, and gadolinium that are combined with ionizing radiation. [1-3] If AuNPs with high- Z target tumor, they can increase the specific absorbed dose with a focus on the tumor, and thereby minimizing the radiation damage to healthy tissues. [4] Lin, et al. used Monte Carlo simulations to differentiate between two types of interaction: nanoparticle interactions on the photons and protons, respectively; they found that the former increased more significantly than the latter. [5] Lin, et al. presented a biological model in which protons require NPs with higher concentrations compared to photons to have the same effectiveness. [6] Butterworth et al., Porcello et al., [7] and Jane et al. [8]. Investigation on simulations of gold (Au), silver (Ag) and platinum (Pt), confirmed that these materials are compatible with each other to participate in treatment. [9] Gao and Zheng studied on MC simulation, in which they simulated a water phantom on a GNP. They concluded that the production of secondary electrons is increased with reducing of proton energy.

Kewon et al. simulated AuNPs in water. [10] In addition, they proposed a radial dose distribution with respect to secondary electrons. They noticed that the effect of AuNPs increased more than a few micrometers in length and a few nanometers in radius direction, respectively [11]. In this study, we used the

MCNPX.2.6 simulator while employing the technique of pencil beam to radiate the proton toward the PB for the first time. As a matter of fact, the absorbed dose and other quantities were examined in two cases: when AuNPs were not injected into the PB, and when AuNPs were injected into it with selecting four concentrations: 10, 25, 50,75 ml/mg. Since that the Coulomb scattering effect is one of the important physical phenomena, we determine the mean scattering angle for these cases, and compare the results**.**

In this work, we use the MCNPX.2.6 code simulator for the first time with the proton irradiation method to the suggested PB, so that we can determine the absorbed dose and the related various quantities (mass stopping power, proton beam deposited energy, generated secondary particles flux, absorbed dose, spread out of Bragg's peak, MCS, CSDA range and straggling proton range) in this phantom in the following two steps. In the first step, AuNPs are not injected into the tumor, while in the second step, AuNPs with the suggested concentrations above are injected into the tumor.

Metods

Stopping power and absorbed dose

The energy loss of ions in a material is the main factor for determining the ions distribution. Because the ion energy (*E*) is lost at at the penetration depth (*x*), where x is the distance inside the target, which is measured from the target level, the lost energy in a material is called stopping power, which is represented by dE/dx. An energetic ion penetrating into a material essentially loses energy with two ways: a) nuclear energy loss (dE/dX_{nuc}) (b) electronic energy loss (dE/dX_{el}); they are independently examined. Thus, total power(S) is given by:

$$S = \frac{dE}{dx} = \frac{dE}{dx}_{nuc} + \frac{dE}{dx}_{el}. \qquad (1)$$

The equation for the proton stopping power in a material is obtained by the quantum mechanical Bethe's equation [12]:

$$\frac{dE}{dx} = \frac{nz^2e^4}{4\pi\varepsilon_0^2 m_e v^2}\left[\left\{\ln\left(\frac{2m_e v^2}{I}\right)\right\} - \ln\left(1 - {v^2}/{c^2}\right) - {v^2}/{c^2}\right] \qquad (2)$$

Where, *Z* is heavy ion atomic number, *e* is elementary charge, *n* is number of electrons per unit volume of matter, *c* is the speed of light in vacuum, $\beta = v/c$, where v is the ion velocity and c is the light velocity, *I* is the mean excitation potential, ε_0 is vacuum permittivity, and m_e is electron mass. Mass stopping power is obtained by: $\frac{1}{\rho}S = -\frac{1}{\rho}\frac{dE}{dx}$. In Fig.2, we compare the total proton mass stopping power in PB using MCNPX.2.6 simulation for two cases: a) without b) with injecting of different concentrations of AuNPs. The absorbed dose is defined as the mean energy deposited inside the matter by ionizing radiation per unit mass. The absorbed dose is in Gray (Gy) in radiotherapy. It is given by:

$$D = 1.602 \times 10^{-10}.F.\frac{S}{\rho} \qquad (3)$$

Where ρ is the density of the absorber material while F is the number of charged particles (proton) per unit cm^2. Fig.3 compares the absorbed dose of two cases a) with and b) without injecting of AuNPs as a function of the penetration depth at the different of incident PB energies. It should be noted that at this simulation work: $F = 1 \times 10^6 \frac{number\ of\ particles}{cm^2}$.

Multiple Coulomb Scattering

Protons that are able to pass through the material and may be deflected by the nucleus of the atom, and it is known as multiple Coulomb scattering *(MCS*). Both the protons and the nuclei have positive charge, therefore, their interactions are mostly Columbic. Highland's formula calculates the mean scattering angle θ [12, 13]:

$$\theta_0 = \frac{14.1MeV}{pv} z_p \sqrt{\frac{L}{L_R}}\left[1 + \frac{1}{9}\log_{10}\left(\frac{L}{L_R}\right)\right] rad \quad (4)$$

Where p is momentum of proton, $v = \beta$c is proton velocity, L is target thickness, and L_R is radiation length of target material. The radiation length is the distance from which the energy of the radiation particles decreases due to radiation losses as much as e^{-1}= (0.37) coefficient. In Fig 4, we compare the mean Coulomb scattering angle in terms of the proton energy at the range of $1 \leq E$ (MeV) ≤ 250, for the injecting of different concentrations of AuNPs in the BP.

CSDA and Straggling Range

In this work, we use CSDA method to calculate the proton range. The CSDA range is obtained by integrating on the reciprocal of the total stopping power with respect to the energy from E_0 to E_f where they are initial and final proton energy, respectively, which is given by: [14]

$$CSDA\ R = \int_{E_f}^{E_0} \frac{dE}{S_{tot}} \qquad (5)$$

In Fig. 5, the comparison of proton range variations in terms of the proton energy in the range of 3 ≤ E (MeV) ≤250 without and with the injection of AuNPs in the breast tissue is depicted as a diagram. The loss

of energy of an ion inside the matter is a statistical process and it is not definite and the Bethe's equation represents only mean energy loss. This variation was obtained by Bohr, who introduced energy straggling (σ_E):

$$\frac{d\sigma_E^2(x)}{dx} \approx \frac{1}{4\pi\epsilon_0{}^2} e^4 \rho_e \qquad (6)$$

where ρ_e = electron density. This is valid for energy loss that is large enough for maintaining Gaussian approximation but it is small enough when its energy can be assumed to be constant. Schulte et al. introduced the following differential equation: [15]

$$\frac{d\sigma_E^2(x)}{dx} = K(x) - 2\frac{dS\big(E(x)\big)}{dx}\sigma_E^2(x) \qquad (7)$$

where K(x) is represented as:

$$K(x) = z^2 \rho_e K \frac{1 - \frac{1}{2}\beta^2}{1 - \beta^2} \qquad (8)$$

range straggling (σ_R), as a function of energy, is determined through the solution of the following equation:

$$\frac{d\sigma_R^2}{dx} = \frac{1}{S(E)}\frac{d\sigma_E^2(x)}{dx} \qquad (9)$$

where $S(E)$ = the total mass stopping power.

Suggested right BP containing tumor

Monte Carlo simulations were done using MCNPX (Monte Carlo N-particles extension) version 2.6, which can handle the interaction and transport of protons, neutrons, electrons, and other particles over a wide range of energies. In the current study, to investigate the analytical phantom of the human body, based on ORNL publications, ORNL female phantom was used to create the input file for MCNPX transport code. Figure 10 illustrates the scheme of this phantom. In the original ORNL phantom, the breast tissue was considered as soft tissue, and for all soft tissues, a unique material had been used. However, it is well known that the material composition of breast tissue is different from other soft tissues. Hence, the breast material was improved. The composition of breast material used in the current study for the suggested ORNL phantom is presented in Table 1. The spherical tumor is located at a radius of 0.5 cm and at a depth of 3 cm from the breast (Figure 1). Note that according to the coordinates shown in Figure 10, the coordinates of the center of the selected tumor are x = -10 cm , z = 52 cm and y = -10 cm which we have simulated using this code. By properly squeezing the breast, the tissue is evenly expanded, its thickness is reduced, and the irradiated time is reduced. The defined source is a single energy point source that is irradiated at a distance of 0.5 cm from the phantom perpendicular to the breast and in the direction of the tumor from 52 to 65 MeV energy with a step of 1 MeV and finally to calculate the absorbed dose in terms of penetration depth in the tumor range was used from Cartesian mesh with a thickness of 1 mm.

Then, we would transport the PB at the range of 3≤E (MeV) ≤250 toward the phantom, and would examine the effect of this beam on the breast tumor. The source defined in this work is a circle with a radius of 25.0 mm, which has a Gaussian energy distribution, and it is close to the phantom. In this work, we insert NPs into tumor tissue using a mechanical injection method. Simultaneously, by injecting AuNPs into cancerous tissue, a PB irradiates the phantom. Then we estimate the absorbed dose in which belong to the two states: i) without and ii) with injection of AuNPs with PB radiation. Finally, we confirm the effect of increasing the absorbed dose in the tumor by injection of NPs.

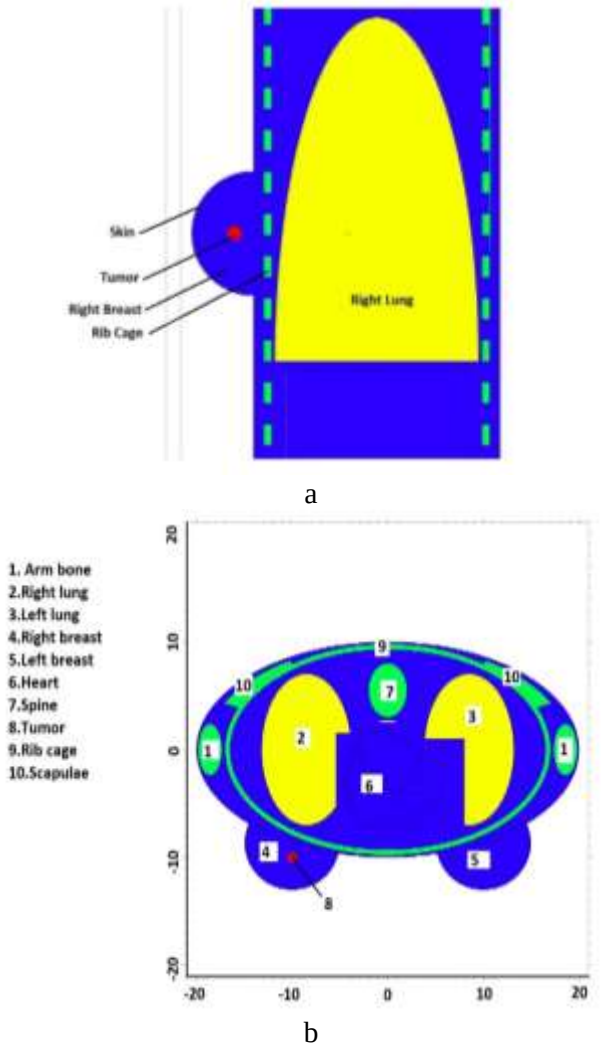

Figure 1 – a) Frontal view of the right breast phantom b) display of Cartesian coordinates of the selected right breast phantom containing a spherical tumor of 1 cm in diameter with adjacent tissues.

Table 1 – Percentage of human tissue components in all phantoms except the infant

lung	skeleton	Soft tissue	element
10.134	7.337	10.454	**H**
10.238	25.475	22.663	**C**
2.866	3.057	2.49	**N**
75.752	47.893	63.525	**O**
0	0.025	0	**F**
0.184	0.326	0.112	**Na**
0.007	0.112	0.013	**Mg**
0.006	0.002	0.03	**Si**
0.08	5.095	0.134	**P**
0.225	0.173	0.204	**S**
0.266	0.143	0.133	**Cl**
0.194	0.153	0.208	**K**
0.009	10.19	0.024	**Ca**
0.037	0.008	0.005	**Fe**
0.001	0.005	0.003	**Zn**
0.001	0.002	0.001	**Rb**
0	0.003	0	**Sr**
0	0	0.001	**Zr**
0	0.001	0	**Pb**
0.296	1.4	1.04	**Density(g/cm$^{3)}$)**

Enhancement of Radiotherapy with Injection of AuNPs to the Tumor

In targeted cancer treatment, physicians use drugs that can better penetrate cancer cells to diagnose and treat [16,17]. For this purpose, AuNPs are used as a photon active element simultaneously with PB irradiation. Radiation therapy by mixing NPs increases the number of photoelectrons in the tumor due to the presence of particles with a high atomic number. As the absorption of photoelectrons into the irradiated tumor increases, the absorbed dose of the tumor increases. Experimental studies have shown that the size of NPs and how they are distributed in different organs are related to each other. The maximum accumulation of AuNPs with diameters of 20-100 and 220 nm is in the liver or spleen, but NPs smaller than 10 nm in diameter were observed in most organs including kidney, heart, lung, brain, liver and spleen. NPs used in medicine are classified into two main groups. The first group of particles that contain organic molecules as the main building material and the second group that usually contain metals and minerals as the core [18,19], NPs (e.g. AuNPs) are commonly used simultaneously with particle therapy to kill cancer cells due to their compatibility with the biological system and their low toxicity. One of the most important parameters of NPs is the choice of their synthesis method. The physical and chemical properties of the particles depend on their synthesis method and the method is selected according to the type of coating agent, appropriate stabilizer and desired size. In order to use AuNPs biologically, their surface must be functionalized, which is called functionalization. The functionalization of NPs is done with the aim of smartening, insensitivity of the immune system and reducing toxicity in the body.

Depending on the application of functionalized NPs, different agents and compounds are used. For example, AuNPs can be functionalized with poly-ethylene glycol to reduce toxicity, escape from the immune system and as a result we have a longer durability in the bloodstream [8]. Another important feature of AuNPs is their easy coupling with antibodies. Therefore, AuNPs are injected into the patient's body in various ways, such as intravenous injection or injection at the tumor site. Inside a healthy tissue, endothelial cells have a regular arrangement and an impenetrable distance for NPs, while in a tumor tissue, the arrangement of endothelial cells is irregular and has large pores, which causes high NPs of gold permeability to tumor tissue. In this process, the antibodies first guide the NPs to the target cells and after they attach to the target cells, they are irradiated. All cancer cells interact with the NPs and are killed by the heat generated with the collision of electromagnetic waves caused by the radiation of a particle beam with AuNPs.

Results and Discussion

In figures 1 to 9 we represent the results of the total mass stopping power, proton deposited energy, secondary particles flux, absorbed dose, spread out of Bragg's peak, mean Coulomb scattering angle, CSDA and straggling range in terms of proton energy at the range of $3 \leq E(MeV) \leq 250$ in breast tissue through MCNPX.2.6 simulation for a: with and b: without injecting of AuNPs, respectively.

As shown in Fig.2 by increasing proton energy, the stopping power is reduced, while with increasing the concentration of AuNPs, the value of this quantity is enhanced. This is due to the density effect and also the production of secondary electrons, which means that collisions respect to distance between the charged particles and the atomic electrons are influenced by their atom interference. These atoms are polarized in the electric field of the charged particles so that the electric field of the electron is reduced in the distance from collision. Since the relativistic effects highlight the collisions with distance, this effect can be clearly seen at the high energy levels. This effect depends on the number of polarized atoms per volume and, consequently, on the density of the materials, and therefore they are called the density effect. Typically,

the ratio of the mass stopping power changes slowly in two materials with the particle energy. Also, if one of the material is solid and the other one is liquid or gas, this ratio will change due to reduce of mass stopping power for solid when the particle energy approaches the relativistic limits.

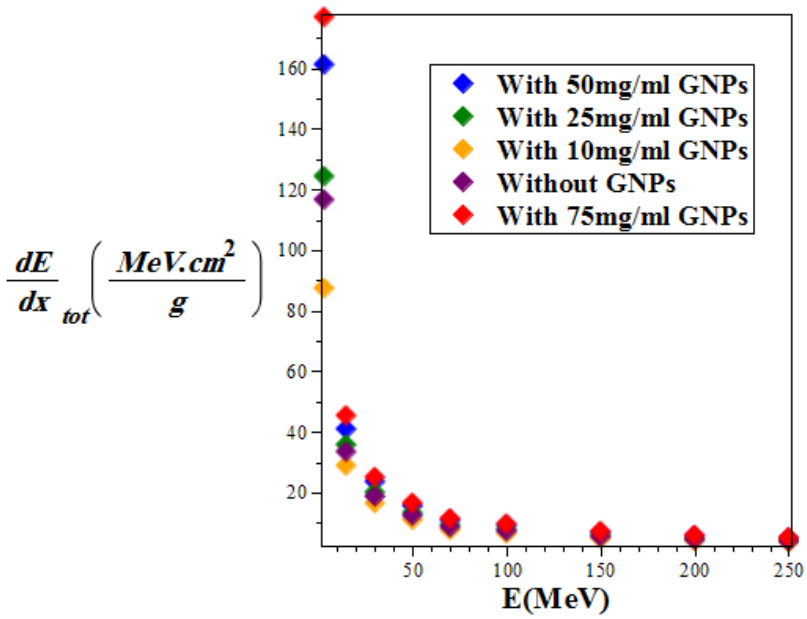

Figure 2 – Comparison of total mass stopping for with/without injection of AuNPs for different concentrations at BP

According to the numbers in Table 1 and the selected phantom, the energy variations of the proton beam in terms of spatial changes x and y in breast tissue containing a spherical tumor with 1 cm diameter for both without and with injecting AuNPs into the tumor are given in Fig3a and b. According to these figures, it can be seen that a proton beam in the direction of the tumor is irradiated from outside to the tumor and its maximum deposited energy at the end of the tumor as it is seen in the dark red region. As can be seen from these figures, the adjacent tissues around the tumor inside the breast are also irradiated to less proton radiation, the color range of which is yellow to orange. The tissues farther behind the tumor (part of the breast tissue, chest, right lung, etc.) receive less deposited energy, their color range is from blue to green, as well as areas that are farther away from the tumor, the amount of deposited energy is equal to zero inside it, and this area is shown in white. From comparing these figures, we see that with injecting AuNPs into the tumor with the amount of 75mg/ ml, the deposited energy increases.

When protons are absorbed by nuclei as a result of nuclear interactions, other particles are released as products. These released particles are called secondary particles (for example: protons, deuterons, lighter nuclei such as alpha , recoil nuclei, gamma photons and neutrons). Each of these generated particles transports some of the initial energy. Deuterons and heavier ions carry much smaller amounts of dose. In total, they make up about 1% or less of the therapeutic absorbed dose, and their energy and range are very small, and they discharge their kinetic energy in a localized manner and very close to their point of origin. Therefore, the dose of secondary particles such as neutrons, electrons, alphas and protons was evaluated here for without and with injecting AuNPs (see Figs 4 and 5).

From the observation of these figures, it can be found that with ingecting AuNPs up to 75mg/ml, the flux of generated secondary particles such as electrons , alphas , protons and neutrons are increased respect to without of AuNPs injecting.

In Figures 6a and b, the diagrams of the varations of absorbed doses in tumor-containing breast tissue are given in terms of the penetration depth of the proton beams for different energy of the incident beam in the range of 52 to 65 MeV for two cases of without/ with injection of AuNPs. As can be seen from these figures, in the energy range of the proton beam, the absorbed dose into the tumor occurs, and with increasing the energy of the proton beam, the absorbed dose into the tumor decreases with increasing penetration depth into the tumor. Injection of AuNPs in the amount of 75 mg/ ml increases the absorbed dose compared to the noninjection mode.

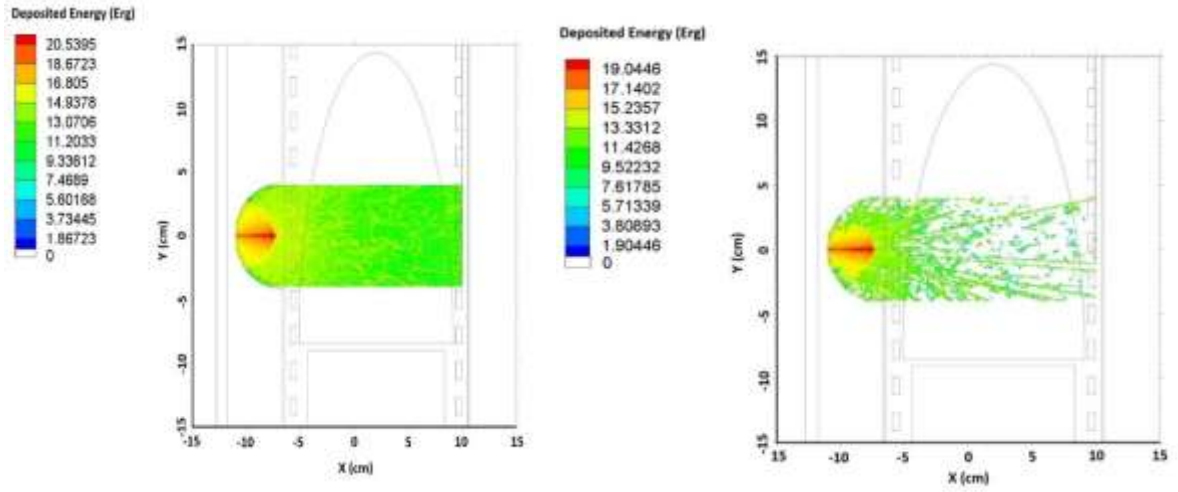

a b

Figure 3 – Deposited energy by the PB for : a) without and b) with injection of AuNPs, (75ml/ mg) in terms of x and y variations in the right breast tissue containing the tumor

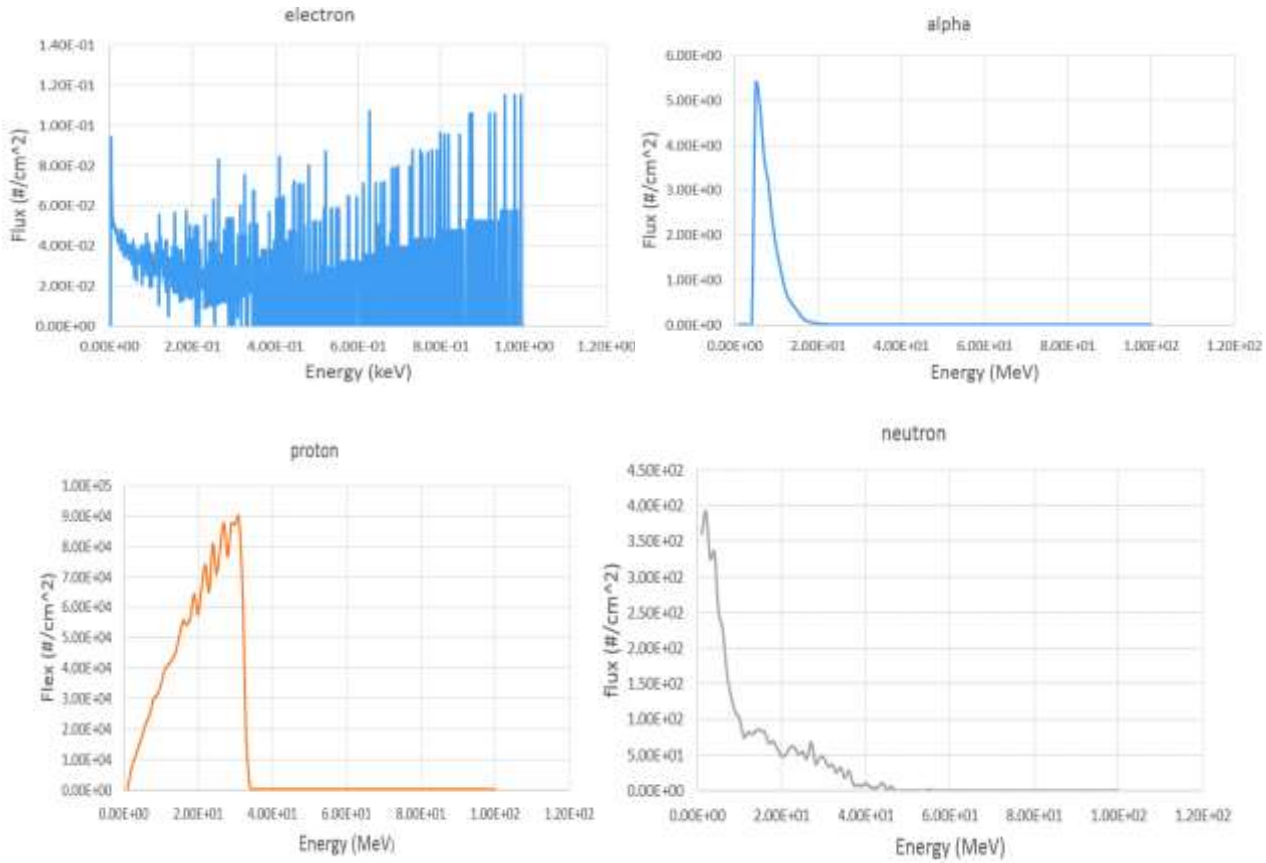

Figure 4 – Flux variations of generated secondary particles for electrons , alphas , protons and neutrons in terms of their energy of these particles without injection of AuNPs.

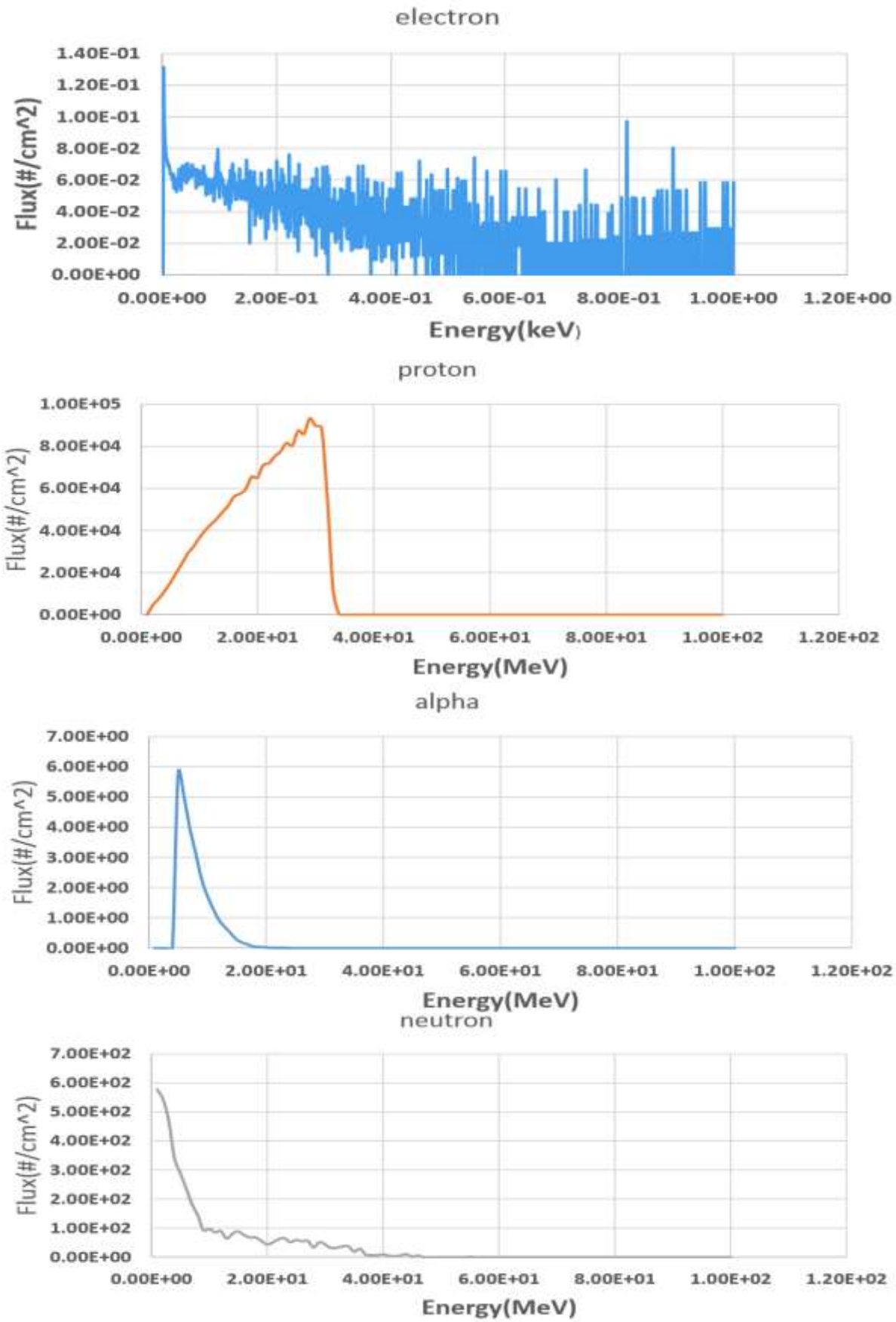

Figure 5 – Flux variations of generated secondary particles for electrons , alphas , protons and neutrons in terms of their energy of these particles with injection of AuNPs.(75mg/ ml)

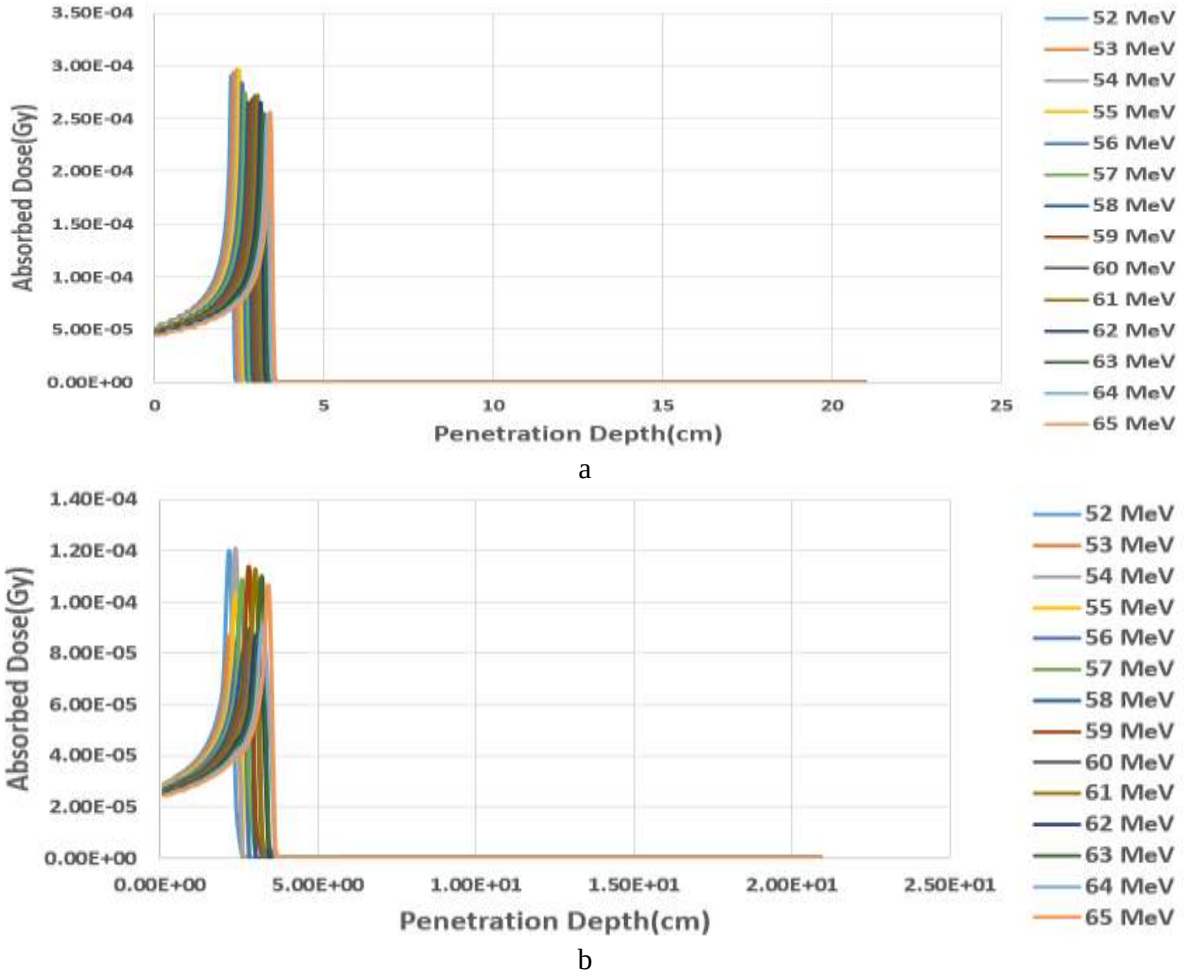

Figure 6 – Variations of absorbed doses into breast tissue containing tumor in terms of penetration depth of the proton beams for different energies of incident beams (each beam contains 10^6 protons) a) without b) with injection of AuNPs.

In order to find the proper range of energy to completely cover the tumor volume, the beam energy was increased step by step. Since Bragg's peaks are narrow on their own and are not suitable for covering any target, the spread out of Bragg's peaks was formed. For this purpose, the number of peaks required to participate in the construction of the spread out of Bragg's peak was calculated until a uniform and maximum dose is delivered to the tumor. Therefore, in Figures 6a and b, we show the diagram of the variations of the spread out of Bragg's peak in terms of the penetration depth of PB inside the breast tissue containing the tumor for without and with the injection of AuNPs. Such that at a depth of penetration of 3 to 4 cm, i.e. within a spherical tumor with a diameter of 1 cm, the spread out of Bragg's peak occurs.

As it can be seen in Fig.7, if the incident PB energy increases, the magnitude of θ_0 will increase in all states; however, the minimum θ_0 in the breast tumor is related to noninjection of AuNPs whereas this amount is gradually increased when the injected concentration of NPs is increased into breast tumor.

By comparing Figures 7a and b, it can be seen that the range of the spread out of Bragg's peak increases with the injection of AuNPs.

As it is shown in Fig.8, without injecting of AuNPs has the highest CSDA range, and it is slightly decreased when AuNPs are increasingly injected so that CSDA range will be approached to its minimum amount of concentration of 75 mg/ml.

As it is shown in Fig. 10, range straggling is increased with the enhancement of proton energy for with/without AuNPs. But the maximum value of this quantity is devoted to the absence of AuNPs injection and the minimum amount of straggling range is related to the injection of 75 mg/ ml AuNPs. This means that with increasing the amount of AuNPs injection, the straggling range is reduced.

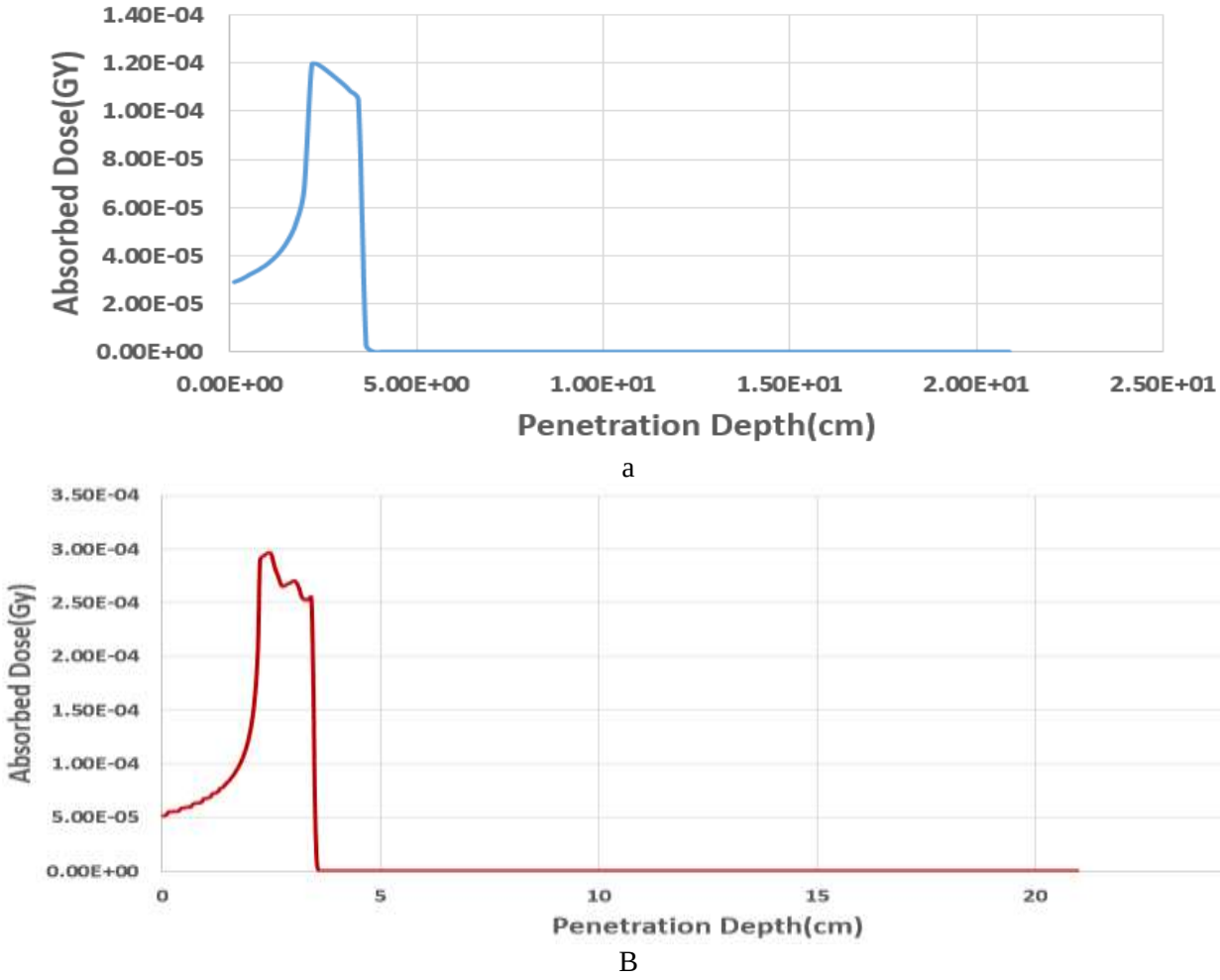

Figure 7 – Variations of the spread out of Bragg's peak in terms of penetration depth of the proton beam into the breast tissue containing tumor a) without b) with injection of AuNPs.

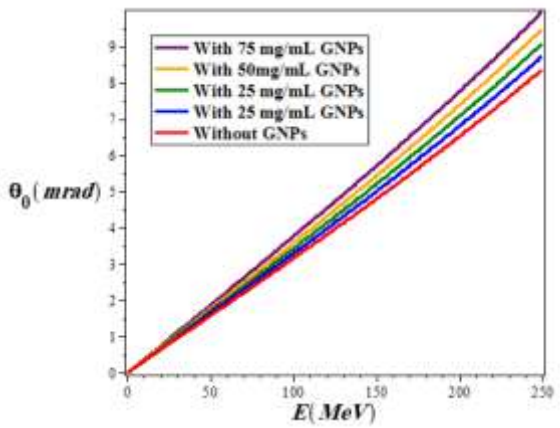

Figure 8 – Comparison of the mean Coulomb scattering angle in terms of proton energy in the range of $3 \leq E\ (MeV) \leq 250$ for the injecting of different concentrations of AuNPs in the PB.

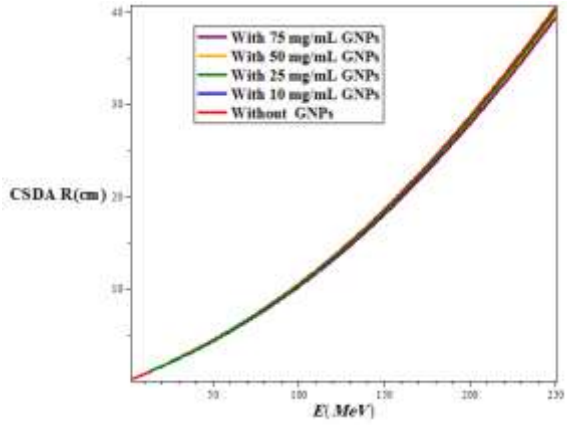

Figure 9 – CSDA range variations for with / without NPs injecting as a function of incident PB energy.

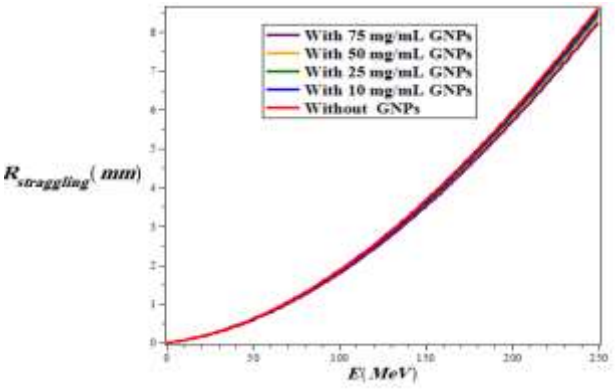

Figure 10 – The comparison between variations of range straggling versus proton energy in the range of $3 \leq E\ (M\text{eV}) \leq 250$ (with/without AuNPs in the breast tissue)

Conclusion

In this work, the MCNPX.2.6 simulation code was used in the treatment of a given tumor inside the BP. Due to the depth of the tumor, the appropriate range of proton energy to cover it was 52 to 65 MeV. The proton absorbed dose in other tissues of the body was lower than the absorbed dose received by the tumor. The flux of secondary particles in healthy organs is much smaller than those of protons received by the tumor, but it is better not to ignore it because the secondary particles release a lot of their energy before reaching the tumor, which can be a risk factor. All of these cases confirm the benefits of proton therapy for primary and non-surgical cancers, but the side effects of generated secondary particles, especially neutrons, are higher than those of other secondary particles and have a higher relative biological effect than electrons and alpha, and by creating more ionization can have a more destructive effect on cells. Therefore, more studies are needed. Also, the results of our simulations show that the injection of AuNPs up to a maximum of 75 mg/ml increases the absorbed dose within the tumor and increases the secondary particles produced, which improves the treatment of breast cancer.

References

1 Ahmad R., Royle G., Lourenço A., Schwarz M., Fracchiolla F., Ricketts K. Investigation into the effects of high-Z nano materials in proton therapy // Phys. Med. Biol. – 2016. – Vol. 61. – P. 4537–4550. DOI: 10.1088/0031-9155/61/12/4537

2 Lacombe S., Porcel E., Scifoni E. Particle therapy and nanomedicine: state of art and research perspectives // Cancer Nano. – 2017. – Vol. 8. – P. 9. DOI: 10.1186/s12951-017-0281-5

3 Kuncic Z., Lacombe S. Nanoparticle radio-enhancement: principles, progress and application to cancer treatment // Phys. Med. Biol. – 2018. – Vol. 63. – P. 02TR01 (27pp). DOI: 10.1088/1361-6560/aaa8a3

4 Kim J.-K., Seo S.-J., Kim H.-T., Kim K.-H., Chung M.-H., Kim K.-R., Ye S.-J. Enhanced proton treatment in mouse tumors through proton irradiated nanoradiator effects on metallic nanoparticles // Phys. Med. Biol. – 2012. – Vol. 57. – P. 8309. DOI: 10.1088/0031-9155/57/24/8309

5 Lin Y., McMahon S.J., Scarpelli M., Paganetti H., Schuemann J. Comparing gold nanoparticle enhanced radiotherapy with protons, megavoltage photons and kilovoltage photons: a MC simulation // Phys. Med. Biol. – 2014. – Vol. 59. – P. 7675–7689. DOI: 10.1088/0031-9155/59/24/7675

6 Lin Y., McMahon S.J., Paganetti H., Schuemann J. Biological modeling of gold nanoparticle enhanced radiotherapy for proton therapy // Phys. Med. Biol. – 2015. – Vol. 60. – P. 4149. DOI: 10.1088/0031-9155/60/10/4149

7 Butterworth K.T., Wyer J.A., Brennan-Fournet M., Latimer C.J., Shah M.B., Currell F.J., Hirst D.G. Variation of strand break yield for plasmid DNA irradiated with High-Z metal nanoparticles // Radiat. Res. – 2008. – Vol. 170. – P. 381–387. DOI: 10.1667/RR1286.1

8 Porcel E., Liehn S., Remita H., Usami N., Kobayashi K., Furusawa Y., Le Sech C., Lacombe S. Platinum nanoparticles: a promising material for future cancer therapy? // Nanotechnology. – 2010. – Vol. 21. – P. 085103. DOI: 10.1088/0957-4484/21/8/085103

9 Jain S. et al. Gold nanoparticle cellular uptake, toxicity and radiosensitisation in hypoxic conditions // Radiother. Oncol. – 2014. – Vol. 110. – P. 342–347. DOI: 10.1016/j.radonc.2013.12.021

10 Gao J., Zheng Y. MC study of secondary electron production from gold nanoparticle in PB irradiation // Int. J. Cancer Ther. Oncol. – 2014. – Vol. 2. – P. 1–7. DOI: 10.14319/ijcto.0201.5

11 Kwon J. et al. Dose distribution of electrons from AUNPs by PB irradiation // Int. J. Med. Phys. Clin. Eng. Radiat. Oncol. – 2015. – Vol. 4. – P. 49. DOI: 10.4236/ijmpcero.2015.42006

12 Newhauser W.D., Zhang R. The physics of proton therapy // Phys. Med. Biol. – 2015. – Vol. 60. – P. R155–R209. DOI: 10.1088/0031-9155/60/8/R155

13 Highland V.L. Some practical remarks on multiple scattering // Nucl. Instrum. Methods. – 1975. – Vol. 129, no. 2. – P. 497–499.

14 Ulmer W., Schaner B. Foundation of an analytical proton beamlet model for inclusion in a general proton dose calculation system // Radiat. Phys. Chem. – 2011. – Vol. 80.

15 Schulte R. et al. Conceptual design of a proton computed tomography system for applications in proton radiation therapy // IEEE Trans. Nucl. Sci. – 2004. – Vol. 51. – P. 866–872.
16 Boylestad L.R., Nashelsky L. Electronic Devices and Circuit Theory. – Upper Saddle River, NJ: Prentice-Hall, 2012.
17 Urban L. A model for multiple scattering in Geant4. – Tech. Rep., 2006.
18 Lewis H. Multiple scattering in an infinite medium // Phys. Rev. – 1950. – Vol. 78, no. 5. – P. 526.
19 Goudsmit S., Saunderson J. Multiple scattering of electrons // Phys. Rev. – 1940. – Vol. 57.

References

1 R. Ahmad, G. Royle, A. Lourenço, M. Schwarz, F. Fracchiolla, and K. Ricketts, Phys. Med. Biol. 61, 4537–4550 (2016).
2 S. Lacombe, E. Porcel, and E. Scifoni, Cancer Nano 8, 9 (2017).
3 Z. Kuncic and S. Lacombe, Phys. Med. Biol. 63, 02TR01 (2018).
4 J.-K. Kim, S.-J. Seo, H.-T. Kim, K.-H. Kim, M.-H. Chung, K.-R. Kim, and S.-J. Ye, Phys. Med. Biol. 57, 8309 (2012).
5 Y. Lin, S. J. McMahon, M. Scarpelli, H. Paganetti, and J. Schuemann, Phys. Med. Biol. 59, 7675–7689 (2014).
6 Y. Lin, S. J. McMahon, H. Paganetti, and J. Schuemann, Phys. Med. Biol. 60, 4149 (2015).
7 K. T. Butterworth, J. A. Wyer, M. Brennan-Fournet, C. J. Latimer, M. B. Shah, F. J. Currell, and D. G. Hirst, Radiat. Res. 170, 381–387 (2008).
8 E. Porcel, S. Liehn, H. Remita, N. Usami, K. Kobayashi, Y. Furusawa, C. Le Sech, and S. Lacombe, Nanotechnology 21, 085103 (2010).
9 S. Jain et al., Radiother. Oncol. 110, 342–347 (2014).
10 J. Gao and Y. Zheng, Int. J. Cancer Ther. Oncol. 2, 1–7 (2014).
11 J. Kwon et al., Int. J. Med. Phys. Clin. Eng. Radiat. Oncol. 4, 49 (2015).
12 W. D. Newhauser and R. Zhang, Phys. Med. Biol. 60, R155–R209 (2015).
13 V. L. Highland, Nucl. Instrum. Methods 129, 497–499 (1975).
14 W. Ulmer and B. Schaner, Radiat. Phys. Chem. 80, (2011).
15 R. Schulte et al., IEEE Trans. Nucl. Sci. 51, 866–872 (2004).
16 L. R. Boylestad and L. Nashelsky, Electronic Devices and Circuit Theory (Prentice-Hall, Upper Saddle River, NJ, 2012).
17 L. Urban, Tech. Rep. (2006).
18 H. Lewis, Phys. Rev. 78, 526 (1950).
19 S. Goudsmit and J. Saunderson, Phys. Rev. 57, (1940).

Article history:
Received 27 January 2025
Accepted 11 March 2025

Мақала тарихы:
Түсті – 27.01.2025
Қабылданды – 11.13.2025

Information about authors:

Seyedeh Nasrin Hosseinimotlagh – Department of Physics, Shiraz Branch, Islamic Azad University, Shiraz, Iran; e-mail: nasrinhosseinimotlagh@gmail.com
Abuzar Shakeri – Department of Physics, Shiraz Branch, Islamic Azad University, Shiraz, Iran; e-mail: nasrinhosseinimotlagh@gmail.com

Авторлар туралы мәлімет:

Сейеде Насрин Хосейнимотлаг – Физика кафедрасы, Ислам Азад университетінің Шираз филиалы, Шираз қ., Иран; e-mail: nasrinhosseinimotlagh@gmail.com
Абузар Шәкери – Физика кафедрасы, Ислам Азад университетінің Шираз филиалы, Шираз қ., Иран; e-mail: Abuzar.shakeri6845@gmail.com